EURASIAN PHYSICAL TECHNICAL JOURNAL

2026, Volume 23, No. 1 (55)

https://doi.org/10.31489/2026N1/15-23

Received: 30/09/2025 Revised: 20/01/2026 Accepted: 19/03/2026 Published online: 30/03/2026

Research Article

UDC 539.374.1, 539.381, 539.4.012, 621.735.3:621.983.31

STUDY OF THE INFLUENCE OF INTERNAL STRESSES ON THE MICROSTRUCTURE OF COATINGS DURING ELECTROLYTIC RUBBING

Gimaltdinov I.[1], Sadykov M.[1], Adigamov N.[1], Kalimullin M.[1], Voinash S.[2], Vornacheva I.[3], Malikov V.[4]

[1] Kazan State Agrarian University, Kazan, Russian Federation
[2] RUDN University, Moscow, Russian Federation
[3] South-West State University, Kursk, Russian Federation
[4] Altai State University, Barnaul, Russian Federation

*Corresponding author: osys11@gmail.com

Abstract. *The paper studies the effect of residual stresses on the microstructure and mechanical properties of metal coatings formed by electrolytic rubbing. The dependence of the internal stress level on the current density, anode rotation speed, electrolyte composition and deposited layer thickness is established. It is shown that with an increase in current density from 50 to 100 A/dm² and a deposition rate of up to 16.6 μm/min, residual stresses vary within 23–34 kg/mm². The addition of ascorbic acid, nickel and manganese chlorides promotes an increase in stresses by 5–10% and simultaneously increases the microhardness of the coatings. A decrease in residual stresses is noted upon reaching a layer thickness of 0.03–0.04 mm, followed by stabilization at a level of 10–12 kg/mm². The results of the work can be used to optimize technological modes of restoration and hardening of agricultural machinery parts, ensuring increased accuracy and quality of metal coatings.*

Keywords: residual stresses, microstructure, elastic deformation, anode, cathode, deposited layer.

1. Introduction

The process of restoring agricultural machinery parts using electrolytic rubbing allows for the formation of metal coatings with specified physical and mechanical properties. However, during the deposition of the metal layer, residual stresses arise in the coating, which significantly impact its performance characteristics, including strength, hardness, and adhesion. The magnitude and nature of these internal stresses are determined by a combination of process parameters, the most important of which are current density, electrolyte composition, substrate geometry, and anode rotation speed [1, 2, 3]. Residual stresses can be either positive or negative. Compressive stresses prevent crack propagation and increase the durability of the coating, while tensile stresses increase the risk of failure. During the manufacturing process, materials undergo uneven deformation due to external influences such as uneven mechanical strain, temperature changes, or phase transitions. Uneven deformation often results in residual stresses [4]. Residual stresses have a significant impact on the strength and other mechanical properties of products and can cause defects such as deformations and cracks during use; these defects ultimately impact the condition of the products and their service life. Therefore, strength analysis and deformation prediction during processing, as well as the assessment of future residual stresses, are pressing issues in modern industrial and scientific research [4].

Theoretical and experimental studies have shown that residual tensile stress deteriorates the fatigue life of a component [5]. Xiao et al. [6, 7] modeled the parameters of residual stress during the study of the grinding process of the surface of a titanium part and also conducted studies on the formation mechanism of residual stress. Huang et al. [8] proposed methods to study the grinding process during the abrasive process, and the residual stress of the workpiece surface after processing was determined during the experiments. Li et al. [9] used molecular dynamics methods to simulate the grinding process of single-crystal silicon. They were able to describe the distribution of residual stress after grinding, and it was also found that reducing subsurface damage during grinding can improve the service life of the workpiece. Wang et al. [10] analyzed the influence mechanism of residual compressive stress on the occurrence of fatigue cracks, estimated the residual compressive stress as a negative load and found that the presence of residual compressive stress reduces the actual average stress of the workpiece and plays an important role in delaying the occurrence of fatigue cracks. Wang et al. [10] analyzed the mechanism of influence of residual compressive stress on the growth of fatigue cracks and found that the presence of residual compressive stress can significantly reduce the intensity of crack formation in the workpiece.

Experiments conducted show that factors limiting the effect of residual stress on fatigue life exist [11, 12]. The conducted modeling can be used to study residual stress and its effect on fatigue life. However, most residual stress simulations can only simulate the formation of residual stress during processing [13] and cannot describe the full mechanism by which residual stress influences fatigue life. An improved technique based on recording the deformations of cylindrical samples and mathematical modeling of the electrolytic process for the precise quantitative determination of residual stresses and stress control has been developed [14-16].

The aim of this study is to analyze the influence of process parameters on the level of residual stresses in order to rationalize the electrolytic rubbing process and improve the quality of restored metal coatings.

2. Materials and Methods

The residual stresses in electrolytic coatings were determined using a method based on recording the elastic deformation of a sample cathode with controlled geometry, allowing for a quantitative assessment of the level of internal stresses in the layer being formed. A cylindrical sample cathode with a given diameter is shown in Figure 1. The prepared sample is placed in a cylindrical housing, after which an anode is installed in the device. Galvanic deposition of metal is performed on the inner surface of the sample cathode, which allows for reproducing the actual conditions of coating formation and conducting a subsequent analysis of the residual stresses that arise [17,18].

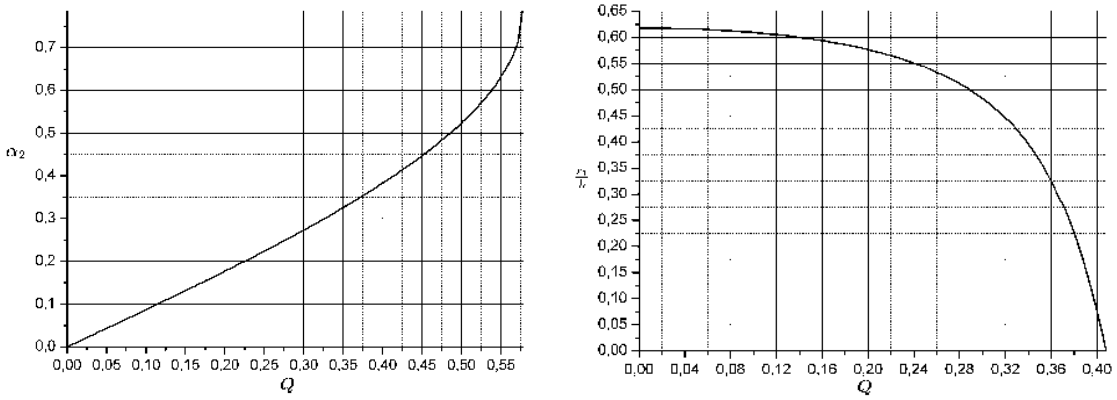

a b

Fig.1. a) Sample assembled with cathode inside cylinder; b) Cathode-sample

After the coating had been deposited and cooled, the substrate (cathode sample), Figure 2, was removed, resulting in elastic deformation of the sample under the action of internal (residual) stresses in the deposit. The resulting deflection was characterized by the value f, measured along the centerline of the cylinder cross-section. To determine the residual stresses in the coating, a classical assumption was used, according to which the internal stresses in the deposit are modeled by an equivalent system of external (reverse) stresses capable of causing similar deformation in the absence of other effects [19,20]. This makes it possible to use the

superposition principle to derive a calculation formula that establishes a relationship between the measured deflection and the level of residual stresses in the coating.

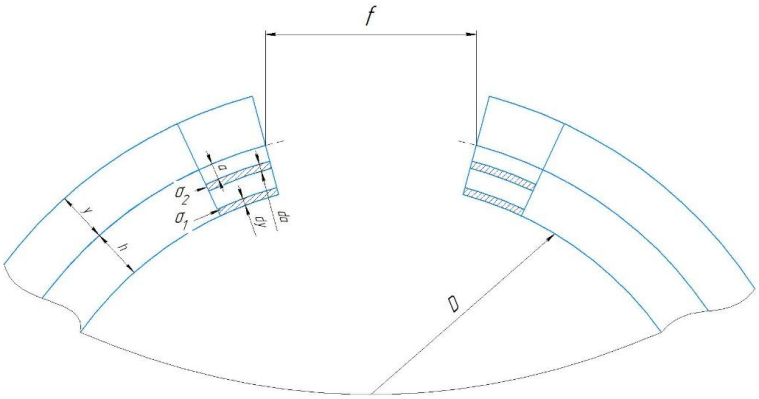

Fig.2. Scheme for calculating residual stresses in coatings

In the process of successive build-up of the coating, when a layer of thickness *da* is deposited, its own stresses are formed in it σ_1 (a). The application of a subsequent layer of thickness dy leads to a change in the stress state in the previously formed layers of the coating. As a result of this, the stresses in the layer located at a distance a from the rod-coating interface consist of two components: primary σ_1 (a), arising directly during the deposition of this layer, and additional σ_2 (a), caused by the action of subsequent layers.

$$\sigma_{tot}(a) = \sigma_1(a) + \sigma_2(a). \quad (1)$$

When a coating element of thickness *da* is deposited, stresses arise in it $\sigma_1(a)$, creating a bending moment about the neutral axis. Because the attitude (h+a)/R0=0.33≤10, the position of the neutral axis can be taken to coincide with the geometric axis of the section. Then the elementary bending moment is determined by the expression:

$$dM = \frac{1}{2}\sigma_1(a)b(h+a)da. \quad (2)$$

According to solid mechanics, the increment of bending moment can be described through the change in the lock opening using the following relation:

$$dM = \frac{E \cdot I_x}{2\pi R^2} df, \quad (3)$$

where E is the modulus of elasticity,

I_x- axial moment of inertia equal to

$$I_x = \frac{b(h+a)^3}{12}, \quad (4)$$

df- increment of the lock solution.

Representing (4) in (3) and assuming that (3) is equal to (2), we obtain

$$\sigma_1(a) = \frac{E}{12\pi R^2} \cdot \frac{df}{da}(a). \quad (5)$$

Deposition of a layer of thickness dy, located at a distance y from the rod-coating interface and characterized by stress σ1(y) leads to the occurrence of a bending moment $dM(y)$ and axial force $dN(y)$, affecting the cross-section at the level (h+y).

$$dM(y) = \frac{1}{2}\sigma_1(y)b(h+y)dy, \quad (6)$$

$$dN(y) = \sigma_1(y)b \cdot dy \quad (7)$$

Bending moment that occurs $dM(y)$ leads to the formation of additional stresses in the previously deposited layer of thickness da

$$d\,\sigma_{2M}(a) = \frac{dM(y)\cdot 12}{b(h+y)^3}\cdot\frac{h-y+2a}{2}, \tag{8}$$

taking into account expression (6), equation (8) can be transformed to the following form:

$$d\sigma_{2M}(a) = \frac{12}{b(h+y)^3}\cdot\frac{h-y+2a}{2}\cdot\frac{1}{2}\sigma_1(y)b(h+y)\cdot dy = \sigma_1(y)\cdot 3\cdot\frac{h-y+2a}{(h+y)^2}dy. \tag{9}$$

Tension $\sigma_1(y)$, included in equation (9) is defined similarly and has the following form:

$$\sigma_1(y) = \frac{E}{12\pi R^2}(h+y)^2\cdot\frac{df}{dy}(y). \tag{10}$$

In this case, expression (9), taking into account (10), is transformed to the following form:

$$d\sigma_{2M}(a) = \frac{E}{12\pi R^2}(h+y)^2\cdot 3\cdot\frac{h-y+2a}{(h+y)^2}\cdot\frac{df}{dy}(y) = \frac{3E(h-y+2a)}{12\pi R^2}\cdot\frac{df}{dy}(y). \tag{11}$$

Total change in stress in the layer da due to the action of a bending moment $dM(y)$ equals:

$$\sigma_{2M}(a) = \int_0^a d\,\sigma_{2M}(a) = \frac{3E}{12\pi R^2}\int_0^a (h-y+2a)df = \frac{3E}{12\pi R^2}\left[(h+a)f(a) + \int_0^a f(y)dy\right]. \tag{12}$$

Under the action of axial force $dN(y)$ in a layer da additional stresses are formed

$$\sigma_{2N}(a) = \frac{dN(y)}{b(h+y)}. \tag{13}$$

Taking into account expressions (7), (13) will take the form:

$$\sigma_{2N}(a) = \frac{\sigma_2(y)dyb}{b(h+y)}. \tag{14}$$

Substituting expression (10) for $\sigma_1(y)$ we will receive:

$$d\sigma_{2N}(a) = \frac{E(h+y)^2}{12\pi R^2(h+y)}\cdot\frac{df}{dy}dy. \tag{15}$$

Total voltage changes $\sigma_{2N}(a)$ in a layer da equals:

$$\sigma_{2N}(a) = \int_0^a d\,\sigma_{2N}(a) = \frac{E}{12\pi R^2}. \tag{16}$$

Total stress in the layer da arising under the action of a bending moment $dM(y)$ and axial force $dN(y)$ is defined by the following expression:

$$\sigma_{2N}(a) = \sigma_{2M}(a) + \sigma_{2N}(a) = \frac{3E}{12\pi R^2}\left[(h+a)f(a) + \int_0^a f(y)dy\right] + \frac{E}{12\pi R^2}\left[(h+a)f(a) - \int_0^a f(y)dy\right] = \frac{E}{12\pi R^2}\left[4(h+a)\cdot f(a) + 2\int_0^a f(y)dy\right]. \tag{17}$$

Total stress in the layerda equals:

$$\sigma_{tot}(a) = \sigma_1(a) + \sigma_2(a) = \frac{E}{12\pi R^2}(h+a)^2\frac{df}{da}(a) + \frac{E}{12\pi R^2}\left[4(h+a)\cdot f(a) + 2\int_0^a f(y)dy\right] = \frac{E}{12\pi R^2}\left[(h+a)^2\frac{df}{da}(a) + 4(h+a)\cdot f(a) + 2\int_0^a f(y)dy\right]. \tag{18}$$

Thus:

$$\sigma_{tot}(a) = \frac{E}{12\pi R^2}\left[(h+a)^2\frac{df}{da}\cdot(a) + 4(h+a)f(a) + 2\int_0^a f(y)dy\right]. \tag{19}$$

Formula (18) describes the stresses in the coating: the first term is the stress from applying the layer *da*, the second and third are stresses from the interaction of this layer with the previous ones and the resulting bending. In the practical part of the study, the substrate was made of sheet iron 0.7 mm thick and 10 mm wide. In all the experiments, the substrate diameter was 120 mm. The thickness of the lining and coating was measured with an accuracy of 0.001 mm. Differential curves were taken for deposition from 0 to 0.1 mm with an interval of 0.01 mm. The deposition time was calculated using the formula and refined experimentally. The standard electrolytic deposition method was used to obtain coatings. Etching of the substrate with nitric acid did not cause additional stresses.

In electrolytically deposited iron films, the dependence of the residual stress on the thickness of the deposited layer demonstrates a pattern similar to that observed in bulk iron samples. Significant internal stresses are formed in the boundary layers directly in contact with the substrate. Depending on the electrolysis parameters, such as current density ($D_к$) and sedimentation rate (V), the magnitude of residual stresses varies in the range from 34 $\frac{\text{kg}}{\text{mm}^2}$($D_к = 150$ $\frac{\text{A}}{\text{dm}^2}$ and V=40 $\frac{\text{ob}}{\text{min}}$) до 23 $\frac{\text{kg}}{\text{mm}^2}$($D_к = 50$ $\frac{\text{A}}{\text{dm}^2}$ и V=20 $\frac{\text{ob}}{\text{min}}$).

When the thickness of the deposited layer reaches 0.03-0.04 mm, a sharp decrease in internal stresses is observed, after which, up to a thickness of 0.1 mm, their insignificant growth is noted. An increase in current density during electrolytic rubbing of iron does not have a significant effect on the magnitude of the internal stresses formed. According to the research data, under stationary conditions of electrolysis at a current density of 50 A/dm^2, in sediments with a thickness of 0.05 mm, internal stresses of the order of 12 kg/mm^2. Application of the anodic-jet deposition method at a similar current density (50 A/dm²) leads to the formation of stresses of the same thickness (0.05 mm) in sediments 12 kg/mm^2. Precipitates obtained by electrolytic rubbing at a current density 150 A/dm^2 and a thickness of 0.05 mm, are characterized by residual stresses equal to 12 kg/mm^2. The difference in the values of residual stresses obtained at different current densities is insignificant.

3. Results and Discussion

The origin of internal stresses in iron electrolytic deposits is associated with a complex of factors. Firstly, it is associated with the absorption of hydrogen, which is released at the cathode simultaneously with iron ions during electro crystallization. Secondly, the mechanism of capture (occlusion) of iron hydroxide particles by the growing metal film plays an important role. Thirdly, the level of internal stresses is affected by increased cathodic polarization observed during iron electrodeposition.

Figure 3 shows a graphical interpretation of the dependence of the cathode deformation (f), expressed in millimeters, on the thickness of the deposited layer (α), measured in micrometers. The abscissa (x) axis shows the values of the deposited layer thickness in the range from 20 to 100 μm, and the ordinate (y) axis shows the corresponding values of the cathode deformation, varying from 1 to 2 mm. The experimental data are presented on the graph as five discrete points marked with special markers. For clarity, the points are connected by a blue trend line, demonstrating the general tendency of the change in the cathode deformation depending on the thickness of the deposited layer.

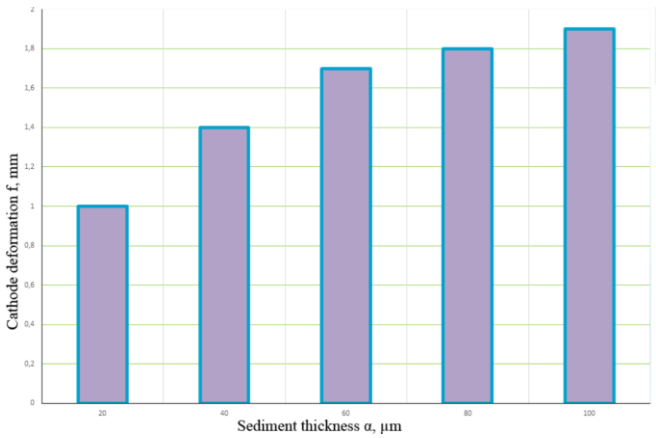

Fig. 3. Dependence of cathode deformation f (in mm) on deposit thickness α (in μm)

The analysis of the presented graphical dependence reveals the presence of a direct correlation between the thickness of the deposited layer and the degree of deformation of the cathode. With an increase in the thickness of the deposited layer, a proportional increase in the deformation of the cathode is observed: from 1 mm at a layer thickness of 20 μm to 1.9 mm at a thickness of 100 μm. The dependence visually observed on the graph has a close to linear character, which indicates a directly proportional relationship between the increase in the thickness of the deposit and the growth of the degree of deformation of the cathode. The obtained results are of high practical importance for the optimization of technological processes associated with the use of cathodes. Knowledge of the nature of the influence of the thickness of the deposited layer on the deformation of the cathode makes it possible to more accurately control the process parameters in order to achieve the specified deformation characteristics.

Figure 4 shows the dependence of the deformation curve (α), crystallization stresses$\sigma_1\ (a)$, tensions, caused by the influence of overlying layers $\sigma_2(a)$ and residual stress $\sigma_{tot}(a)$, from the sediment thickness (α), expressed in micrometers (μm). All types of stress are presented в kg/mm^2. Analysis of graphical data reveals different dynamics of changes in internal stresses depending on the thickness of the deposited layer (α). Residual stress curve $\sigma_{tot}(a)$ shows a sharp decline from 25 кг/мм^2 at α=*0* μm to 10 kg/mm^2 at α=40 μm, after which stabilization is observed in the range 10-12 kg/mm^2. A similar trend, but with a more pronounced decline (от 28 до 2-3 kg/mm^2), characteristic of crystallization stresses $\sigma_1(a)$, in the thickness range from 0 to 40 μm, after which their values also stabilize.

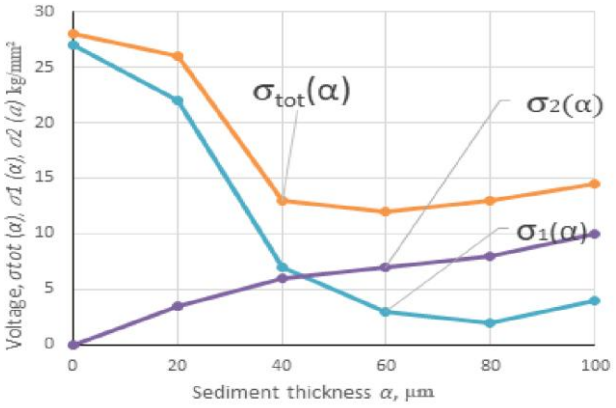

Fig. 4. Deformation curve (a) and corresponding crystallization stresses $\sigma_1(a)$, stresses of the impact of overlying layers $\sigma_2(a)$ and residual stress $\sigma_{tot}(a)$

In turn, the stresses caused by the influence of the overlying layers $\sigma_2(a)$, demonstrate monotonous growth от 0 до 10 kg/mm^2 proportionally to the increase in the thickness of the deposited layer from 0 до 100 μm. Thus, in the initial stages of sedimentation (α <40 μm) the dominant contribution to the formation of the internal stress state is made by crystallization stresses, whereas with further growth of the sediment thickness (α> 40 μm) the determining role is played by the stress induced by the overlying layers. The obtained results are of practical interest for predicting the mechanical behavior of the material and optimizing the technological parameters of deposition in order to achieve the specified properties. The insignificant increase in residual stresses observed in iron deposits obtained by electrolytic rubbing can be explained by a combination of two factors. Firstly, the deposits formed by electrolytic rubbing are characterized by a low tendency to hydrogenation, which minimizes the influence of hydrogen in the formation of internal stresses. Secondly, such deposits, as a rule, have an increased structural defectiveness, in particular, a tendency to form microcracks, which also helps to reduce the level of residual stresses. The effect of such an electrochemical parameter as the current density on the cathode on the value of residual stresses in electrolytic iron obtained by electrolytic rubbing is shown in Figure 5.

In the range of current densities 50–150 A/dm² an increase in residual stresses is observed, but when exceeded 150 A/dm² they are reduced. In thin coatings (0.01 mm, anode speed 20 ob/min) voltage increases from 16.2 to 29.2 kg/mm² with increasing current density, whereas for layers (>0.05 mm) the effect of current density becomes insignificant. In thin layers, residual stresses depend on the substrate, and their relaxation through microcracks is difficult, whereas in thickened layers, stresses relax through microcracks, weakening the dependence on current density at thicknesses >0.04 mm. Iron deposits with residual stresses 12–15 kg/mm²

demonstrate stability due to partial stress relaxation and compensating properties of the material. Increasing the rotation speed of the anode with 20 to 40 ob/min leads to an increase in residual stresses: in thin layers (0.01 mm, 150 A/dm²) with 29.2 to 32 kg/mm², and in thick ones (0.1 mm) with 17.7 to 20 kg/mm². Acceleration of the anode reduces the crystal growth time, forming a fine-grained structure with increased strength and an increase in internal stresses. Refining the grains increases the area of the boundaries between them, facilitating the release of dislocations and the growth of internal tensile stresses.

Figure 6 shows the dependence of residual stresses on the deposit thickness (in the range of 0.05 - 0.1 mm) obtained from electrolytes with various additives. Analysis of the graphical data shows that the introduction of ascorbic acid, manganese chloride and nickel additives leads to an increase in residual stresses in the deposits.

1- 600 g/l $FeCl_2 \cdot 4H_2O$; pH=1; $D_к = 150 \frac{A}{gm^2}; V = 20 \frac{ob}{min}$.

2- 600 g/l $FeCl_2 \cdot 4H_2O$; pH=1; $0{,}5 \frac{g}{l} C_6H_8O_6$; $D_к = 150 \frac{A}{dm^2}; V = 20 \frac{ob}{min}$.

3- 600 g/l $FeCl_2 \cdot 4H_2O$; pH=1; $0{,}5 \frac{g}{l} C_6H_8O_6$; $25 \frac{g}{l} NiCl_2 6H_2O$; $D_к = 150 \frac{A}{dm^2}; V = 20 \frac{ob}{min}$.

600 g/l $FeCl_2 \cdot 4H_2O$; pH=1; $0{,}5 \frac{g}{l} C_6H_8O_6$; $25 \frac{g}{l} MnCl_2 4H_2O$; $D_к = 150 \frac{A}{dm^2}; V = 20 \frac{ob}{min}$.

Addition of ascorbic acid to the electrolyte reduces layering and cracking in the deposits, increasing residual stresses due to improved mechanical properties.

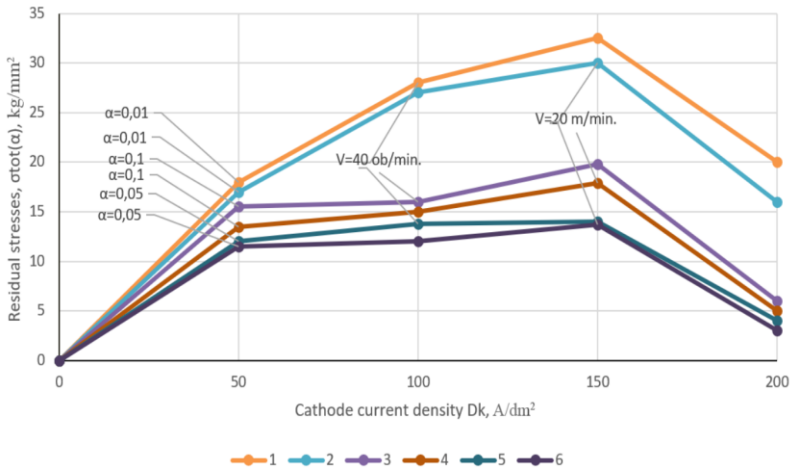

Fig. 5. Effect of cathode current density on residual stresses in iron deposits at different deposit thicknesses and anode rotation speeds

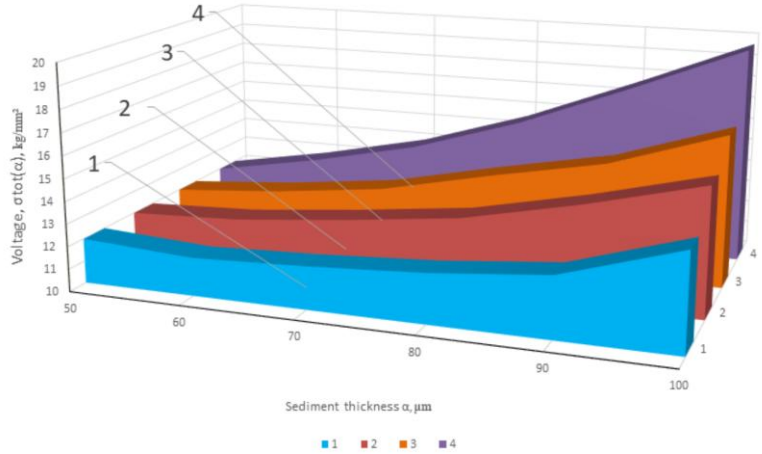

Fig. 6. Dependence of residual stresses on sediment thickness

Additions of nickel and manganese chlorides increase residual stresses due to the formation of chemical compounds during ion discharge, simultaneously improving the mechanical properties of the deposits. A slight

increase in stresses from the additives is compensated by an increase in microhardness and an improvement in the results of the technological bending test.

4. Conclusion

The study demonstrated a significant influence of residual stresses on the properties of coatings obtained by electrolytic rubbing. It was found that at a current density of 50–100 A/dm² residual stresses vary from 23 to 34 kg/mm² depending on the sedimentation rate and layer thickness. When the sediment thickness reaches 0.03–0.04 mm, the stresses decrease sharply and then stabilize at the level 10–12 kg/mm². Additives to the electrolyte, such as ascorbic acid, nickel and manganese chlorides, increase residual stresses by 5–10%, while improving the microhardness and strength characteristics of the deposits. The proportional increase in cathode deformation, varying from 1 to 1.9 mm with an increase in the layer thickness from 20 to 100 μm, indicates a linear relationship between the deposited layer thickness and the stress state. The data obtained allow us to more accurately predict the mechanical behavior of the coatings and optimize the deposition process parameters.

Conflict of interest statement

The authors declare that they have no conflict of interest in relation to this research, whether financial, personal, authorship or otherwise, that could affect the research and its results presented in this paper.

CRediT author statement

Gimaltdinov I.: Conceptualization, Methodology; **Sadykov M. and Adigamov N.:** Software; **Kalimullin M. and Voinash S.:** Validation; **Vornacheva I**.: Writing - Review & Editing; **Malikov V**.: Supervision.
The final manuscript was read and approved by all authors.

Acknowledgements

The work was supported by a grant (No. 143/2024 - PD dated 16.12.2024) to young candidates of science (postdoctoral students) with the aim of defending a doctoral dissertation, performing research work, and performing labor functions in scientific and educational organizations of the Republic of Tatarstan.

References

1 Sadykov M., Gimaltdinov I., Adigamov N., Zagidullin R., Zalyakaeva D. (2024) Theory and practice of substantiation of electroplating modes by electrolytic rubbing. *AIP Conf. Proc.*, 3154, 020054. DOI: 10.1063/5.0201265.

2 Sadykov M.R., Gimaltdinov I.Kh. (2024) Restoration of machine parts by electrolytic rubbing. *L. Machinery and equipment for the village*, 324, 37-41. https://doi.org/10.33267 / 2072-9642-2024-6-37-41

3 Lee R.I. (2018) Model of contact stresses and durability of metal-polymer roller bearings. *Adhesives. Sealants. Technologies*, 3, 33 – 37. https://doi.org/10.1134/S1995421218040123

4 Jiang G., Haiyang F., Bo P. (2021) Recent progress of residual stress measurement methods: A review. *Chinese Journal of Aeronautics*, 34(2), 54-78. https://doi.org/10.1016/j.cja.2019.10.010

5 Guijian X., Benqiang C. (2022) Fatigue life analysis of aero-engine blades for abrasive belt grinding considering residual stress. *Engineering Failure Analysis*, 131, 105846. https://doi.org/10.1016/j.engfailanal.2021.105846

6 Guijian X., Kangkang S. (2021) Comprehensive investigation into the effects of relative grinding direction on abrasive belt grinding process. *Journal of Manufacturing Processes*, 62, 753-761. https://doi.org/10.1016/j.jmapro.2020.12.073

7 Na X., Weijun H., Yongjian Z. (2020) High cycle fatigue behavior of a low carbon alloy steel: The influence of vacuum carburizing treatment. *Engineering Failure Analysis*, 109, 104215. https://doi.org/10.1016/j.engfailanal.2019.104215

8 Huang Y. (2021) Research progress of aero-engine blade materials and anti-fatigue grinding technology. *J. Aero-Eng. Mater.*, 41(4), 17-35. https://doi.org/10.11868/j.issn.1005-5053.2021.000058

9 Penghui L., Xiaoguang G. (2021) Effects of grinding speeds on the subsurface damage of single crystal silicon based on molecular dynamics simulations. *Applied Surface Science*, 554, 149668. https://doi.org/10.1016/j.apsusc.2021.149668

10 Dharmesh K., Idapalapati S. (2022) Influence of residual stress distribution and microstructural characteristics on fatigue failure mechanism in Ni-based Superalloy. *Fatigue & Fracture of Engineering Materials & Structures*, 44 (5), 159574. https://doi.org/10.1111/ffe.13454

11 Yun H. (2021) Research on the fatigue failure behavior of 1Cr17Ni2 blades ground by abrasive belt with passivation treatment. *Engineering Failure Analysis*, 129, 105670. https://doi.org/10.1016/j.engfailanal.2021.105670

12 Zhang X.C., Zhang Y.K. (2010) Improvement of fatigue life of Ti–6Al–4V alloy by laser shock peening, *Materials Science and Engineering*, 527 (15), 3411-3415. https://doi.org/10.1016/j.msea.2010.01.076

13 Xiangfan N., Weifeng H. (2020) Experimental study and fatigue life prediction on high cycle fatigue performance of laser-peened TC4 titanium alloy. *Materials Science and Engineering: A*, 822, 141658. https://doi.org/10.1016/j.msea.2021.141658

14 Li R.I. (2018) Model of the Contact Stresses and Endurance of Metal–Polymer Roller Bearings. *Polymer Science*, 11(4), 382-386. https://doi.org/10.1134/S1995421218040123

15 Malokhatko E.Yu. (2024) Effect of internal mechanical stresses in a multilayer structure on displacement for various designs of microelectromechanical membranes. *St. Petersburg State Polytechnical University Journal. Physics and Mathematics*, 17, 121-124. https://doi.org/10.18721/JPM.173.223

16 Kablov E.N. (2021) The Influence of Internal Stresses on the Aging of Polymer Composite Materials: a Review. *Mechanics of Composite Materials*, 57 (5), 565-576. https://doi.org/10.1007/s11029-021-09979-7

17 Tkacheva A.V. (2024) Effect of combined thermal action of electric arc welding with aluminothermic backfill on internal stresses in a steel plate. News of higher educational institutions. *Ferrous metallurgy*, 67 (5), 604 – 611. https://doi.org/10.17073/0368-0797-2024-5-604-611

18 Smirnov A.N. (2016) Effect of the degree of deformation of welded joints of carbon steels on the structural-phase state and internal stress fields. *Welding and diagnostics*, 3, 25-28. Available at: https://www.elibrary.ru/item.asp?id=26901508

19 Kuryntsev S.V. (2020) Analysis of the influence of the welding type on the phase composition and internal stresses of welded joints of austenitic and duplex steels. *Science-intensive technologies in mechanical engineering*, 3(105), 3-11. https://doi.org/10.30987 / 2223-4608-2020-3-3-11

20 Gaskarov I.R., Farkhshatov M.N., Saifullin R.N. (2022) Cylindrical interfaces repair technique using electric resistance welding of metal powder materials. *Results in Engineering*, 16, 100699. https://doi.org/10.1016/j.rineng.2022.100699

AUTHORS' INFORMATION

Gimaltdinov, Ildus Khafizovich – Candidate of Technical Sciences, Associate Professor, Acting Head of the Department of Machine Operation and Repair, Kazan State Agrarian University, Kazan, Russian Federation; https://orcid.org/0000-0003-2297-8950; kafedrarm@yandex.ru

Sadykov, Marat Rashitovich – Assistant of the Department of Machine Operation and Repair, Kazan State Agrarian University, Kazan, Russian Federation; https://orcid.org/0009-0003-9335-6080; marat3012@yandex.ru

Adigamov, Nail Rashatovich – Doctor of Technical Sciences, Professor of the Department of Machine Operation and Repair, Kazan State Agrarian University, Kazan, Russian Federation; https://orcid.org/0009-0007-3647-1858; n-adigamov@rambler.ru

Kalimullin, **Marat Nazipovich –** Doctor of Technical Sciences, Associate Professor of the Department of Machine Operation and Repair, Kazan State Agrarian University, Kazan, Russian Federation; https://orcid.org/0000-0001-6867-3103; marat-kmn@yandex.ru

Voinash, Sergey Aleksandrovich – Assistant at the Department of Architecture and Restoration, RUDN University, Moscow, Russian Federation; https://orcid.org/0000-0001-5239-9883; sergeyvoinash@yandex.ru

Vornacheva, Irina Valerievna – Candidate of Technical Sciences, Associate Professor, South-West State University, Kursk, Russian Federation; https://orcid.org/0009-0003-5511-235X; vornairina2008@yandex.ru

Malikov, Vladimir Nickolaevich – Candidate of Technical Sciences, Associate Professor, Department of General and Experimental physics, Altai State University, Barnaul, Altai Territory, Russian Federation; https://orcid.org/0000-0003-0351-4843; osys11@gmail.com